ACS OMEGA

http://pubs.acs.org/journal/acsodf

Article

Vibration Response Analysis of the Tail Beam of Hydraulic Support Impacted by Coal Gangue Particles with Different Shapes

Lirong Wan, Jiantao Wang, Qingliang Zeng, Dejian Ma, Xuehui Yu, and Zhaosheng Meng*

Cite This: *ACS Omega* 2022, 7, 3656−3670

Read Online

ACCESS | Metrics & More | Article Recommendations

ABSTRACT: The existing research on coal gangue identification based on vibration usually assumes that coal gangue particles are ideal shapes. To understand the vibration response difference in hydraulic support caused by coal and gangue with real shapes, this paper uses a three-dimensional (3D) scanning technology to determine the real shape of coal particles. The process of coal and gangue impacting the tail beam at different angles was simulated in the LS-DYNA software package, and the effects of shape parameters, velocity, and coal strength on the difference in vibration signals caused by the two were analyzed statistically. The conclusions are as follows: the vibrational response of the tail beam is concentrated mainly in the area between the ribs. The regularity of the velocity signal caused by gangue is better than the regularity of the velocity signal caused by coal, and the attenuation speed of the acceleration signal of gangue is slower than the attenuation speed of the acceleration signal of coal. The probability distributions of the velocity and acceleration responses were analyzed statistically, and the results show that the results from coal can be well fitted by a logarithmic normal function, and the standard deviations of velocity and acceleration are 0.05591 and 489.8, respectively. The gangue results are fitted by the gamma function and the Weibull function, and the standard deviations are 0.13531 and 737.9, respectively, showing that the fitting function has the potential to be used as the basis for coal gangue identification. The change in coal strength has little effect on the vibration response of the tail beam. With increasingly falling velocity, the vibration signal intensity of the tail beam increases, but the discrimination between coal and gangue weakens; therefore, measures should be taken to reduce the falling velocity of the rock mass. The research results of this paper can provide a reference for further study of coal gangue identification methods based on vibration.

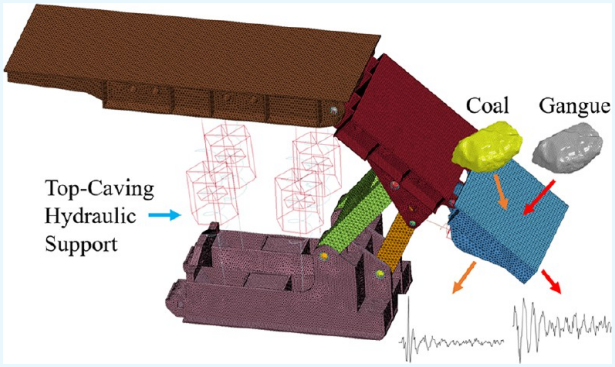

1. INTRODUCTION

There are many important energy sources on earth, such as geothermal energy and natural gas.[1,2] Coal, as an important part of primary energy,[3,4] plays an important role in world energy security.[5,6] The fully mechanized top coal caving technology has obvious advantages in medium and thick coal seams.[7] However, the precise control of the coal caving mechanism is the key to achieving high yield and high efficiency of the fully mechanized top coal caving technology.[8] Therefore, as the basis of the coal caving mechanism, the study of the coal gangue identification technology is of great significance to top coal caving mining. However, the problem of low reliability of coal gangue identification in practical applications is prominent.

Many countries have carried out extensive research on the coal gangue identification technology. At present, the main detection methods include the 3D laser scanning technology, the gamma ray method, the image recognition method, the acoustic signal recognition method, and the vibration signal recognition method. The 3D laser scanning technology needs to be combined with the dynamic weighing technology,[9] and due to the narrow space and poor vision of the coal mining face, the application of this technology is difficult. In the process of top coal caving mining, the dust concentration of the coal caving port is significant, causing great difficulties in the image recognition method.[10−12] Many field signals are doped in the sound signals of the coal caving process, and these field signals need to be eliminated when using the sound signal recognition method.[13] The effectiveness of the gamma ray method has been greatly improved after transforming artificial gamma rays into natural gamma rays,[14] but the sensor is too expensive to be used widely.

The vibration response method is currently one of the most effective methods for coal gangue identification. In the process of top coal caving mining, coal and gangue will impact the tail

Received: November 8, 2021
Accepted: January 6, 2022
Published: January 19, 2022

https://doi.org/10.1021/acsomega.1c06279
ACS Omega 2022, 7, 3656−3670

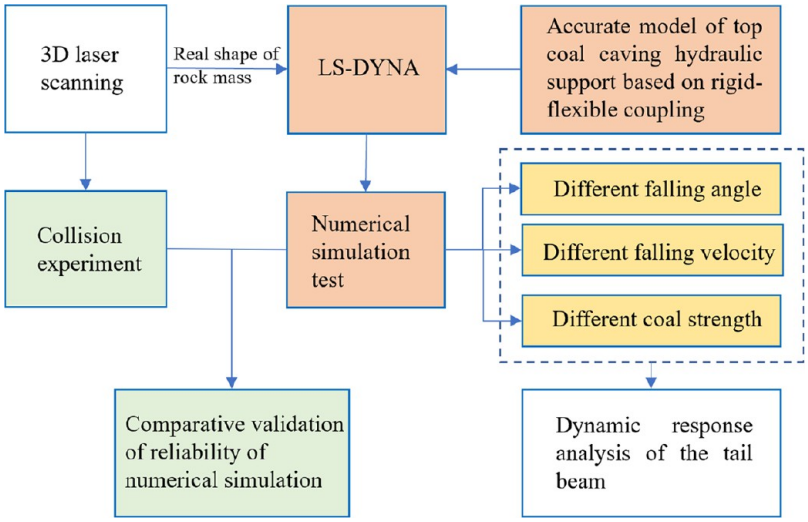

Figure 1. Sketch of the problem.

beam of hydraulic support. Due to the difference in the nature of coal and gangue, the effects of coal and gangue impacting on the tail beam are different. The vibration signal without noise interference can be obtained by the velocity and acceleration sensors installed under the tail beam. Therefore, the degree of falling of coal can be identified by monitoring the vibration of the tail beam.

To study the difference in vibration signals caused by coal and gangue, Zeng et al. explained the propagation of vibration signals in metal plates during collision by analyzing the contact between spherical coal particles and metal plates.[15] Wan et al. found that the change in the material would lead to different vibration responses of the metal plate by simulating the process of spherical coal and gangue impacting the metal plate.[16] Yin et al. established a finite element model of rock impacting metal plates with the same mass and different shapes and found that different shapes of rock would cause different vibration responses.[17] Chen et al. simulated the process of the spherical coal particle impacting the simplified hydraulic support tail beam and found that the impact position and the caving angle had a significant indigenous effect on the dynamic response of the tail beam.[18]

In terms of the influence of the real shape of the rock mass on its dynamic behavior, Yan et al. studied the impact of rock on reinforced concrete sheds by changing the traditional assumption of spherical rock to ellipsoid rock and found that the shape and falling gesture of rock had an obvious influence on the impact effect.[19] By scanning real rock aggregate particles and conducting discrete element numerical simulation tests, Xie et al. found that the bulk density of rock aggregates is related to some shape parameters of rock aggregates.[20] In the study of Lu et al., rockfall particles were modeled as three-dimensional polyhedrons, and the surface area ratio and the length-width ratio of rocks were found to have a quadratic effect on the energy dissipation and trajectory change of rocks.[21] A three-dimensional stochastic discrete element model of soil-rock mixtures with different stone shapes was established by Wang et al. to study the influence of shapes on the macroscopic mechanical properties under different loading methods.[22] Yan et al. proposed a 3D model that focuses on simulating the trajectory of rockfalls under the conditions of rocks and terrain of any shape.[23] Su and Choi studied the cushioning performance of gabion filled with different forms of rocks by the discrete element method and found that rocks with a round morphology could disperse the load more evenly to achieve the best cushioning performance.[24]

In summary, the existing research on coal gangue identification based on vibration ignores the influence of the real shape of the rock mass on the vibration response, and the rock particles are assumed to be the ideal shape. At the same time, the model of a rock mass impacting hydraulic support is simplified to a rock mass impacting the metal plate or tail beam with fixed constraints. However, rock shape has been proven to have an important influence on its dynamic behavior, which proves that the shape of the rock mass has an important influence on the research object. Therefore, the real shape of the rock mass is introduced into the study of coal gangue identification based on vibration, and the real shape of the coal particle is obtained by the 3D scanning technology. The reliability of the coal material model is verified by experiments. The process of the real shape coal and gangue impacting the tail beam was simulated in the LS-DYNA software package, and the difference in the vibration response of the hydraulic support after the impact was compared. The influence of rock shape parameters, velocity, and coal strength on the vibration signal was studied by statistical analysis. The results provide a reference for top coal caving mining and coal gangue identification based on the vibration response. The sketch for this study is shown in Figure 1.

2. RECONSTRUCTION AND SHAPE ANALYSIS OF ROCK PARTICLES

2.1. Shape Acquisition. To determine the real digital geometric parameters of the coal gangue particle surface, according to the technical route shown in Figure 2, the spatial point cloud data characterizing the surface morphology of coal particles were obtained using a 3D laser scanner. Geomagic Studio software was used for postprocessing the point cloud data. The coal particles are divided into tetrahedral mesh by HyperMesh software.

2.2. Shape Description. Different shapes and falling gestures lead to different vibration signals. Shape information for the contact area with the tail beam in coal gangue particles needs to be described by microscopic shape parameters, and the falling gesture is affected mainly by macroscopic shape

https://doi.org/10.1021/acsomega.1c06279
ACS Omega 2022, 7, 3656−3670

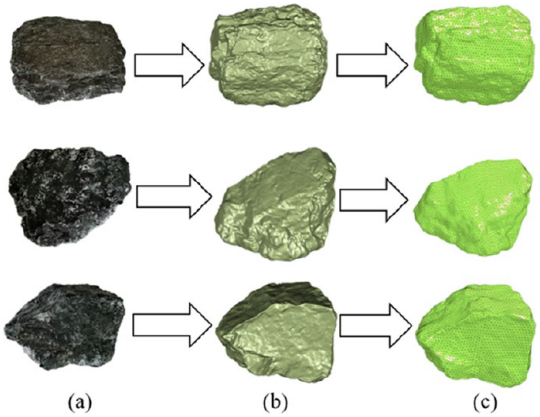

Figure 2. Acquisition process of the 3D shape information for coal. (a) Coal, (b) 3D model, and (c) finite element model.

parameters. According to some related research,[25−27] this paper uses six parameters in two scale ranges to describe the shape of coal gangue particles: elongation index (EI), flatness index (FI), sphericity (ψ), texture (T), equivalent elliptical perimeter ratio (AIPE), and surface fractal dimension (D_s).

In the macroscopic parameters, EI reflects the degree of slenderness of the particle. The larger the EI is, the more slender the particle. FI reflects the degree of flatness of the particle. The smaller the FI is, the flatter the particles. ψ reflects the degree of the particle close to the ball. The larger ψ is, the closer the particles are to the shape of the sphere. EI, FI, and ψ are defined in Formulas 1−3.

$$\mathrm{EI} = \frac{L}{S} \tag{1}$$

$$\mathrm{FL} = \frac{S}{I} \tag{2}$$

$$\psi = \sqrt[3]{\frac{(I \times S)}{L^2}} \tag{3}$$

where L, I, and S represent the lengths of the long axis, middle axis, and short axis of coal particles, respectively.

In the microscopic parameters, D_s and AIPE reflect the angularity of the coal particle, T reflects the surface texture of the coal particle, and D_s, AIPE, and T are defined in Formulas 4−6

$$D_S = 1 + D_P \tag{4}$$

$$\mathrm{AIPE} = P/P_{\mathrm{ellipse}} \tag{5}$$

$$T = P/P_{\mathrm{convex}} \tag{6}$$

where D_P is the surrounding fractal dimension of the coal particle, P is the projection perimeter of the particle contour, P_{ellipse} is the equivalent elliptical perimeter of the particles, and P_{convex} is the convex perimeter of the coal particle.

The images of three angles of each particle in nine particles were collected, and the images were imported into Image-Pro Plus software to measure the above four shape parameters of particles. Finally, the average values of three angles were taken as the values of each parameter of each particle.

The shape parameters of 9 lumps of coal are shown in Table 1.

Table 1. Shape Parameters of Coal Particles

rock label	EI	FL	ψ	texture	D_S	AIPE
1	1.536	0.951	0.7638	1.0306	2.01332	1.0825
2	1.531	0.736	0.8337	1.0164	2.01062	1.0681
3	2.219	0.584	0.7032	1.0114	2.006617	1.038
4	2.083	0.615	0.7207	1.0193	2.00971	1.0612
5	2.42	0.515	0.6919	1.0141	2.00663	1.0597
6	2.213	0.488	0.4184	1.013	2.00904	1.0623
7	2.254	0.487	0.4036	1.0152	2.00752	1.0436
8	2.127	0.733	0.6704	1.0108	2.00661	1.051
9	1.844	0.688	0.4275	1.0223	2.012177	1.0602

3. NUMERICAL MODEL AND EXPERIMENTAL REFERENCE

3.1. Finite Element Model. In this paper, ZF4800-17-32 top coal caving hydraulic support was selected for analysis. Its working resistance is 4800 kN, and the maximum working height is 3.2 m. 3D modeling software is used to establish the model at a ratio of 1:1. The telescopic beam and the insert plate have little effect on the vibration response of the tail beam, which is omitted to simplify the model and improve the calculation efficiency. The mesh of hydraulic support and rock is divided into tetrahedral units, and the total number of elements is 582417. The rotational connection between the components of the hydraulic support is realized by adding a virtual rotational pair. Hydraulic cylinders are ideally assumed to be spring damping systems.[28] In the numerical simulation, the tail beam of the hydraulic support is parallel to the shield beam, and the angle between the tail beam and the ground is 40°. The finite element model of hydraulic support and rock particles is shown in Figure 3.

Preprocessing is carried out in LS-PREPOST, and the velocity of rock particles is 8 m/s. The degree of freedom of the element nodes at the bottom layer of the hydraulic support base is fully constrained. The simulation time is 0.02 s, and the hydraulic support is affected only by gravity. Due to the short collision process, the self-stability process of the hydraulic support under gravity is omitted. The contact between the coal particle and the metal plate is * CONTACT _ ERODING _ SURFACE _ TO _ SURFACE, and the contact algorithm uses the penalty function method.

The components of hydraulic support are mainly welded by steel plates. The piecewise linear plasticity model in LS-DYNA is selected as the material model of the steel plate. This model is an elastic−plastic material, and the strain rate is described by the Cowper and Symonds model. The model combines yield stress and factor.

$$1 + \left(\frac{\dot{\varepsilon}}{C}\right)^{1/p} \tag{7}$$

where $\dot{\varepsilon}$ is the strain rate.

The strain rate and yield stress meet eq 8[29]

$$\sigma_0(\varepsilon_e^P, \dot{\varepsilon}_e^P) = \sigma_0(\varepsilon_e^P)\left[1 + \left(\frac{\dot{\varepsilon}_e^P}{C}\right)\right] \tag{8}$$

where σ_0 is the yield stress limit, ε_e is the effective strain rate, C and P are the strain rate parameters, and $\sigma_0(\varepsilon_p^e)$ is the yield stress.

The material model parameters for metal plates are shown in Table 2.

https://doi.org/10.1021/acsomega.1c06279
ACS Omega 2022, 7, 3656−3670

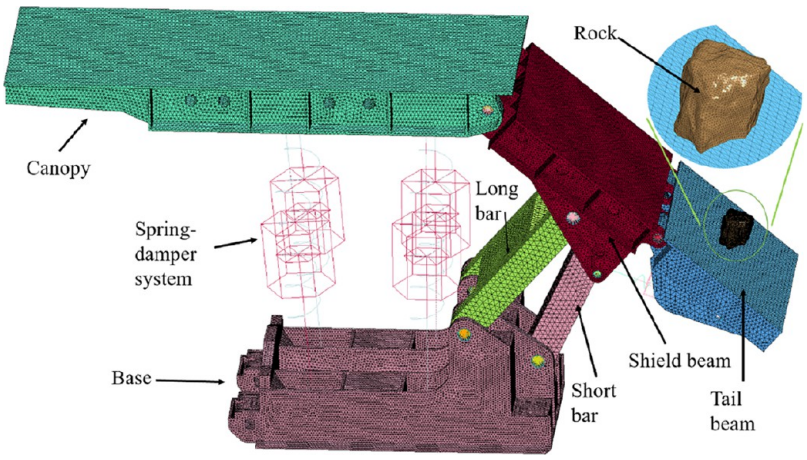

Figure 3. Finite element model of the tail beam of hydraulic support impacted by coal gangue particles.

Table 2. Material Model Parameters of the Metal Plate

ρ(kg/m^3) 7830	E(Pa) 2.07 × 10^{11}	u 0.3	σ_0(Pa) 2.07 × 10^8
C	P	ε_f	
40	5	0.75	

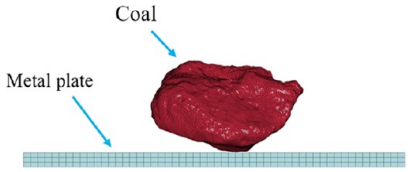

Figure 4. Numerical model for simulating coal drop.

The material model of coal and gangue is * MAT _ JOHNSON _ HOLMQUIST _ CONCRETE (HJC model for short). The HJC model is recognized as a model suitable for simulating the mechanical behavior of brittle rock materials under low-speed collision.[30,31] This model includes three parts: the strength model, damage, and state equation, which can simulate the compressive damage behavior of brittle materials under dynamic loading.[32] The strength and density of gangue are greater than the strength and density of coal. The HJC model parameters of gangue in this paper are shown in Table 3.[33]

3.2. Model Test Verification of the Coal Material. Due to the large degree of crushing in the process of coal impacting the tail beam and in order to ensure the authenticity of the crushing effect of coal in the simulation, we conducted a coal drop test, simplified the model of coal particle impacting the tail beam into coal particle impacting the metal plate, and raised the coal particle on the test bench to 3.3 m away from the bottom metal plate. When falling from this height, the speed before the coal particle contacted the steel plate was approximately 8 m/s. A high-speed camera was used to record the whole process of the coal particle impacting the metal plate.

A coal particle is randomly selected from the coal particles to obtain 3D shape information, and the coal particle is raised to 3.3 m from the bottom plate on the test bench. When falling from this height, the speed of the coal particle before contacting the steel plate is approximately 8 m/s. The high-speed camera was aligned to the steel plate during shooting.

The numerical model of the test is shown in Figure 4. The length, width, and height of the metal plate are 400, 400, and 15 mm, respectively. The nodes around the metal plate are fully constrained. The falling gesture of the coal particle in the numerical model is the same as the falling gesture of the experiment. The mass of the coal particle is 2.4 kg, and the falling speed of the coal particle is 8 m/s. The metal plate adopts the hexahedral element. The contact algorithm and the material model of the metal plate are the same as those in the previous section.

Long et al.[34] divided 18 parameters related to material properties in the HJC model into sensitive parameters and nonsensitive parameters. Nonsensitive parameters use existing data,[35] and then the crushing process consistent with the test is obtained by debugging the sensitive parameters. The failure stress parameter f_c in the HJC model cannot simulate the failure of the material;[33] so in the simulation, the failure of the material is controlled by adding the keyword *MAT_ADD_EROSION. The HJC model parameters for coal are shown in Table 4.

The process recorded by the high-speed camera shows that the crushing process of the coal particle is divided into two main processes: initial contact and secondary contact. After the initial contact of the coal particle, local crushing occurs at the contact position, but no overall fracture occurs. After the initial collision, the coal particle flips in the air and then has a secondary contact with the steel plate. In the secondary contact process, the local crushing of the impact position is accomplished, and the coal particle has an overall fracture. After the first collision, the joints and fractures inside the coal particle were developed but did not develop to run through the whole coal particle. After the secondary contact, the fractures were further expanded, and the coal particle finally produced an overall fracture. Figure 5 shows that the key stage of coal fragmentation is well simulated in the numerical simulation.

Table 3. HJC Model Parameters of Gangue

ρ_0(kg/m^3) 2590	G(Pa) 1.114 × 10^{10}	f_c(Pa) 1.223 × 108	C 0.006	N 0.6	S_{max} 7.7	D_1 0.04	D_2 1	ε_{fmin} 0.01
T(Pa)	p_c(Pa)	μ_c	p_l(Pa)	μ_l	k_1	k_2	k_3	f_s
7.76 × 106	4.075 × 107	0.0023	1.65 × 109	0.11	1.15 × 10^{10}	2.6 × 10^{10}	5 × 10^{10}	0

https://doi.org/10.1021/acsomega.1c06279
ACS Omega 2022, 7, 3656−3670

Table 4. HJC Model Parameters of Coal

ρ0(kg/m3) 1400	G(Pa) 5.8 × 108	f_c(Pa) 9 × 106	C 0.006	N 0.76	S_{max} 7.7	D_1 5 × 10^{-6}	D_2 1	ε_{fmin} 2 × 10^{-6}
T(Pa)	p_c(Pa)	μ_c	p_l(Pa)	μ_l	k_1	k_2	k_3	f_s
1.86 × 106	3 × 106	8 × 10^{-4}	3.4 × 108	0.1	1.6 × 109	−1.7 × 108	5.8 × 109	1.4

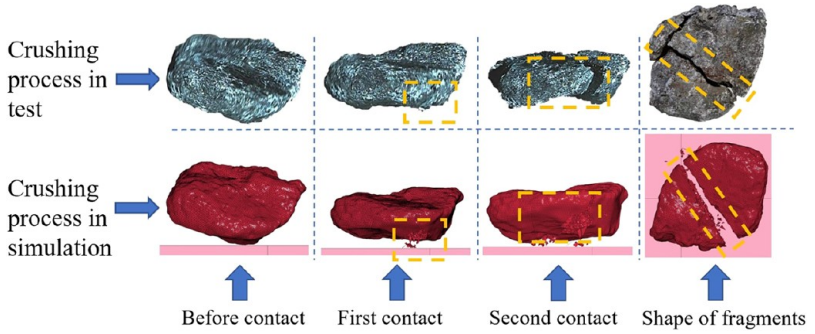

Figure 5. Comparison of the coal crushing process filmed by the camera and numerical simulation process.

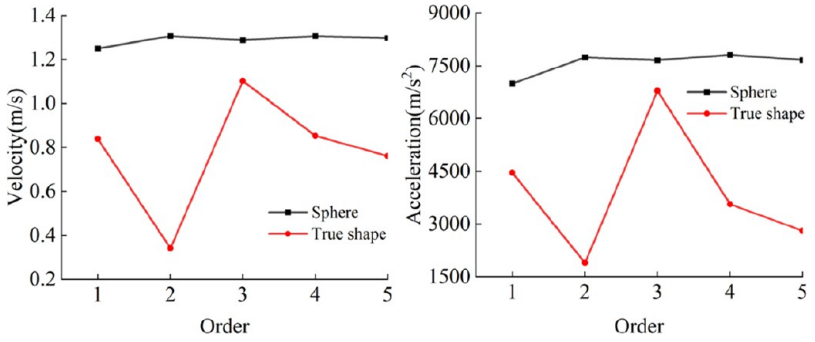

Figure 6. Comparison of velocity and acceleration responses caused by the ideal shape and real shape coal particle.

3.3. Comparison of Real Shape and Ideal Shape. To illustrate the difference between the tail beam vibration signal caused by the real shape particles and the ideal shape, in this section, we design the numerical simulation test of spherical and real shape coal particles impacting the metal plate, and the mass of the two shapes of particles is the same. In each simulation, the particles flipped at a certain angle. The velocity and acceleration signals of the first contact position are extracted, and the effective values in the first 0.01 s are calculated. The test results are shown in Figure 6. When the spherical coal particles impact the metal plate, the change in the velocity and acceleration response of the metal plate can be neglected. However, when the real-shaped coal particle impacts the metal plate, the response of the metal plate shows no obvious regular change because the real shape of the particle surface is more complex. When the rock particles impact the metal plate at different angles, the different falling postures and the surface shapes of the contact area will cause different vibration effects on the metal plate. Therefore, when the tail beam is impacted, the vibration signal generated by the ideal shape of the coal gangue particles and the real shape of the coal gangue particles will also show a greater difference, so it is necessary for the real shape of the coal gangue particles to impact the tail beam vibration characteristics in further research.

3.4. Setting of the Numerical Simulation Test. In this paper, numerical simulation experiments of coal and gangue impact tail beam are carried out. The two groups of experiments use the same nine rock shapes, and all the coal and gangue particles have the same mass. Each rock has fifteen numerical simulations with different angles. Based on the previous angle, the rock particles are rotated 30° with the *XYZ*-axis of the spatial orthogonal coordinate system as the rotation center, which is the second contact angle. The contact angle with the tail beam for 15 tests of a particle is shown in Figure 7.

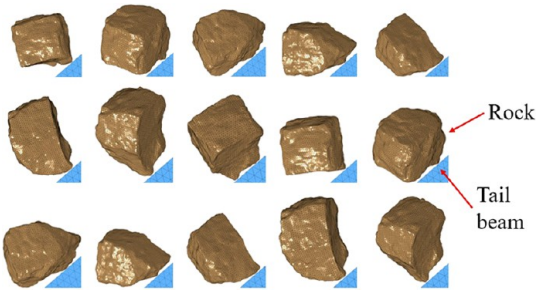

Figure 7. 15 angles of contact of the same rock particle.

4. RESULTS AND DISCUSSION

4.1. Propagation and Waveform Analysis of Vibration. The process of propagation of velocity on the tail beam is shown in Figure 8. After the collision, the disturbance caused by the impact load on the tail beam gradually diffuses outward to form the stress wave. The propagation of the stress wave constantly changes the velocity and acceleration of each point on the tail beam. The change in the state of velocity and acceleration propagates in the form of waves. The velocity wave is limited by a very short time after encountering the rib plate. A long strip

https://doi.org/10.1021/acsomega.1c06279
ACS Omega 2022, 7, 3656−3670

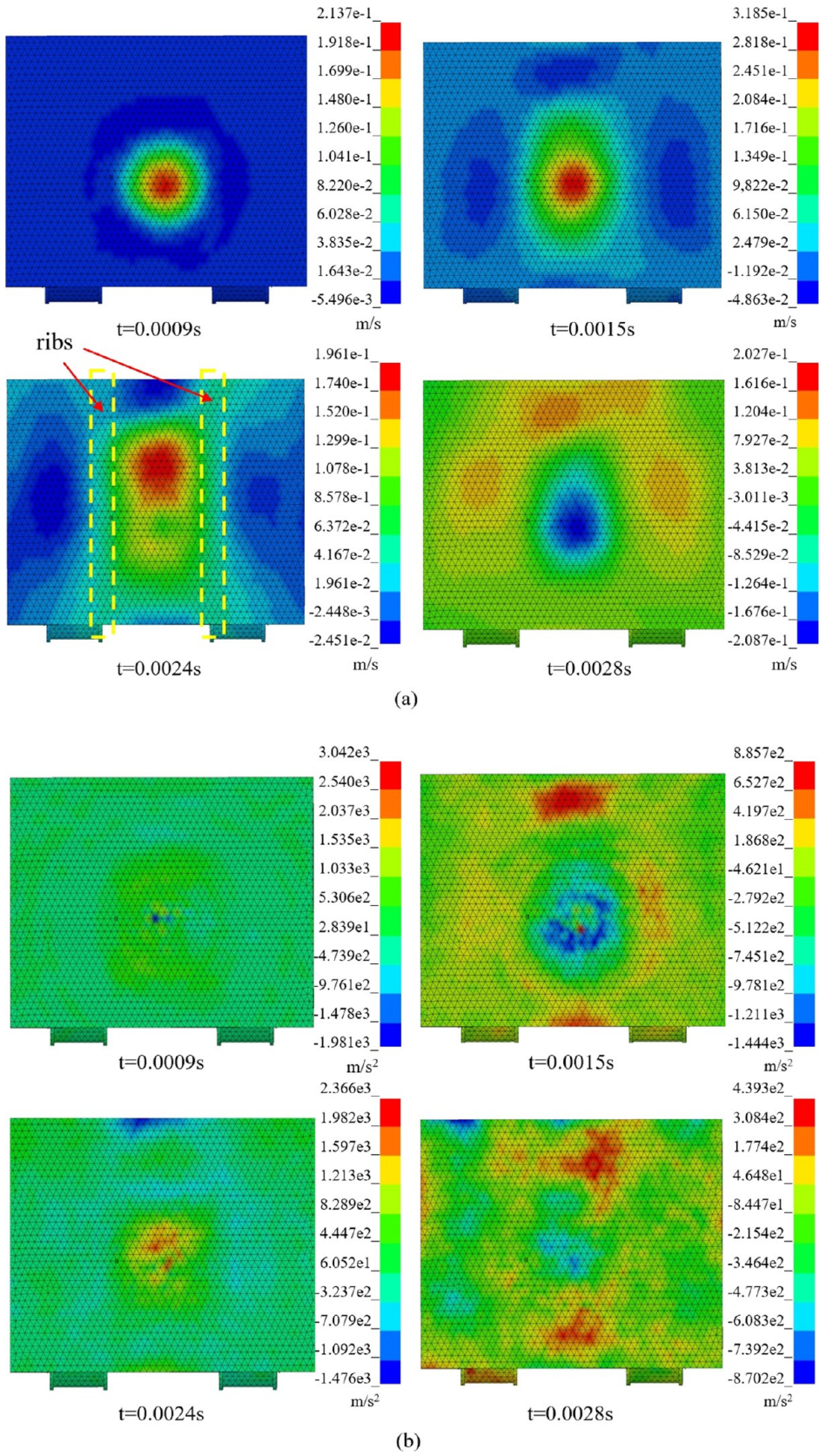

Figure 8. Velocity and acceleration cloud map. (a) Velocity and (b) acceleration.

velocity cloud map filled with space between two rib plates appears on the tail beam, and then the velocity wave passes through the rib plate and causes a wide range of oscillations of the whole tail beam. The propagation process of the acceleration on the tail beam is shown in the diagram. Similar to the velocity, the larger value area is concentrated mainly in the area between

https://doi.org/10.1021/acsomega.1c06279
ACS Omega 2022, 7, 3656−3670

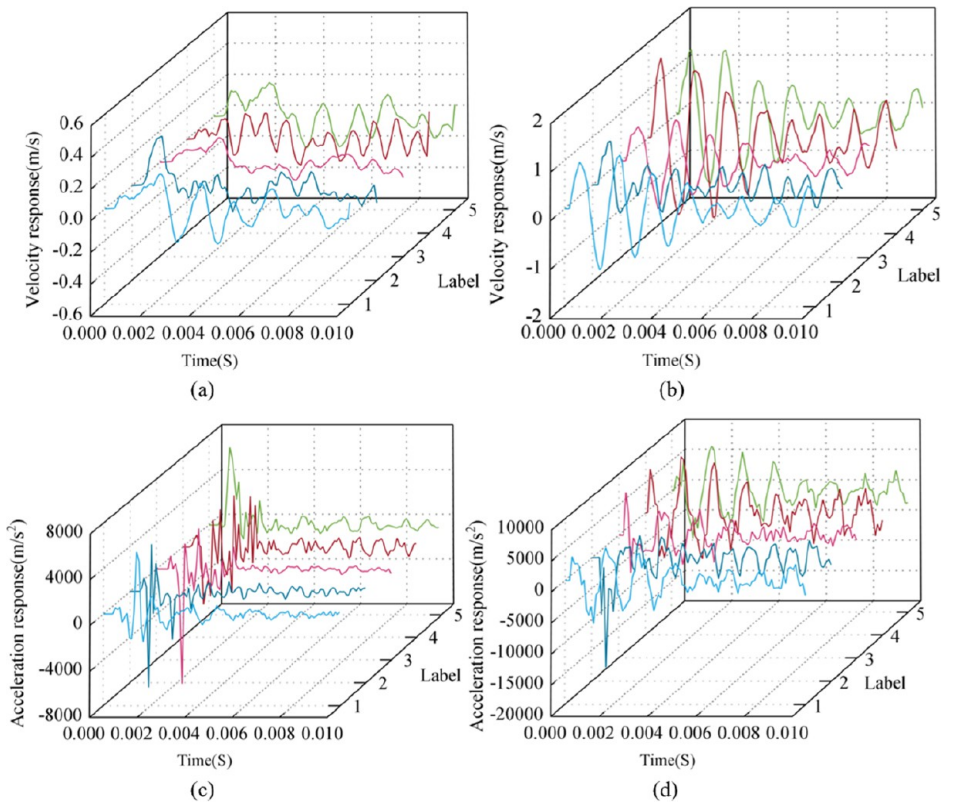

Figure 9. Waveform comparison of coal and gangue. (a,b) Velocity response of coal and (c,d) acceleration response of gangue.

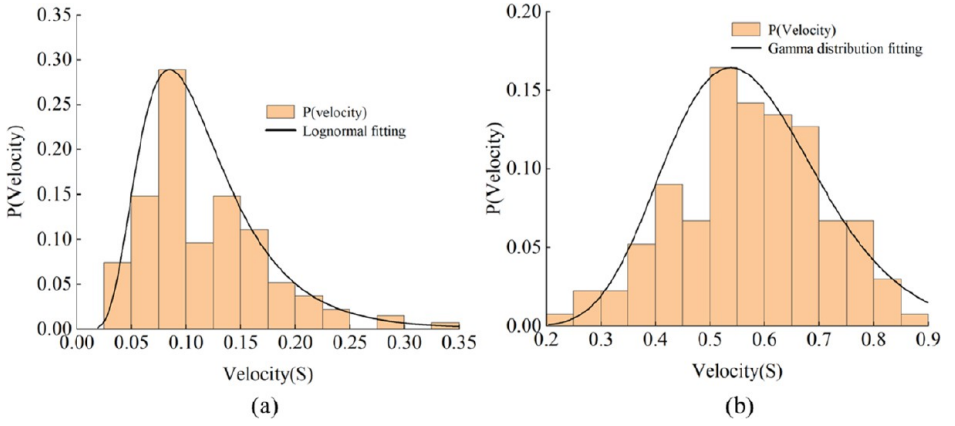

Figure 10. Velocity response probability distribution of coal gangue. (a) Coal and (b) gangue.

the two rib plates, but the propagation speed of the acceleration wave is far greater than the propagation speed of the velocity wave. When t = 0.0015 s, the velocity wave is mainly limited between the two rib plates, and the acceleration has been transmitted to the whole tail beam. Therefore, to detect a strong vibration signal, the sensor should be located away from the stiffened plate.

Figure 9 shows the velocity and acceleration response curves of the tail beam caused by coal and gangue at five different angles under the same shape and mass. In terms of velocity response, the velocity fluctuation amplitude of gangue is significantly higher than the velocity fluctuation amplitude of coal, which may be related to the influence of material properties on the instantaneous energy transfer in collision. Due to the serious fracture of coal and obvious absorption of kinetic energy at the moment of impact, the impact of coal on the tail beam is weakened. In addition, the acceleration response curve of the tail beam impacted by gangue fluctuates smoothly and shows obvious regularity attenuation, but the fluctuation regularity of the coal acceleration curve is poor, possibly caused by serious coal crushing after impact and multiple slip collisions between broken particles and the tail beam.

In terms of the acceleration response, the acceleration fluctuation amplitude of gangue is also significantly higher than the acceleration fluctuation amplitude of coal, and the acceleration attenuation of coal is significantly faster than the acceleration attenuation of gangue, possibly because the energy transmitted by gangue impact is greater than the energy transmitted by coal impact, forming a stronger stress wave, which causes a long-term oscillation of the tail beam.

Therefore, the results show that the velocity and acceleration response of the hydraulic support tail beam after impact on coal

https://doi.org/10.1021/acsomega.1c06279
ACS Omega 2022, 7, 3656−3670

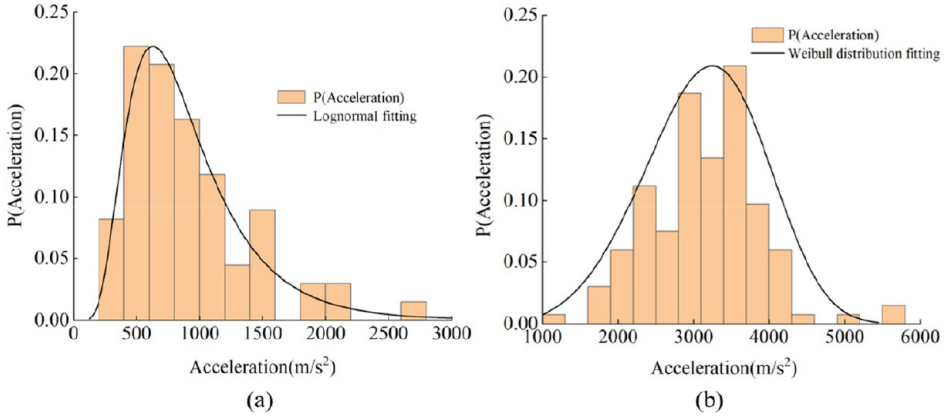

Figure 11. Acceleration response probability distribution of coal gangue. (a) Coal and (b) gangue.

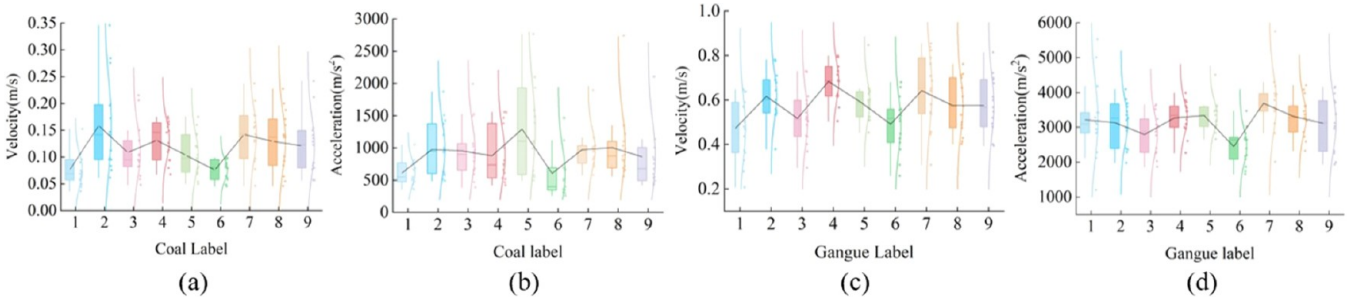

Figure 12. Distribution of response results of rock particles. (a) Velocity distribution of coal, (b) acceleration distribution of coal, (c) velocity distribution of gangue, and (d) acceleration distribution of gangue.

gangue has obvious differences. The results provide a reference for the identification of coal gangue in caving mining.

4.2. Overall and Individual Distribution. Since the sampling time is only 0.01 s, only the time domain analysis of velocity and acceleration signals is carried out. Because the mean value of velocity and acceleration is near 0, this paper chooses the effective value and standard deviation as the parameters to describe the time domain characteristics of the signal. The source of velocity and acceleration data is the area where the tail beam is first impacted by rock particles. In a small area, the velocity change of each node can be ignored, and the acceleration response curve will be quite different. Therefore, the velocity signal of one node and the acceleration signal of four nodes in the collision area are extracted, and then the average value of the effective value of the four nodes of the acceleration signal is calculated.

Taking the effective value of the response signal within the first 0.1 s of the tail beam as the research object, the probability distribution diagram of the velocity response caused by coal and gangue is shown in Figure 10. There are obvious differences between the two materials in the probability diagram. The former follows the lognormal distribution, and the latter follows the gamma distribution. The mean values are 0.11644 and 0.57352, respectively, and the standard deviations are 0.05519 and 0.13531, respectively. The velocity response caused by coal is more concentrated. The probability distribution of the acceleration response caused by coal and gangue is shown in Figure 11. The former obeys a lognormal distribution, and the latter obeys a Weibull distribution. The mean values are 913.03 and 3147.09, and the standard deviations are 489.8 and 737.9, respectively. The acceleration signals caused by coal are more concentrated, indicating that under the same impact energy and contact state, the response caused by gangue is more sensitive to the initial contact state, and the shape change has a greater impact on the signal caused by gangue. At the same time, if coal is continuously mixed with gangue, the curve fitting the probability distribution of the vibration signal may gradually change.

The vibration response of the tail beam is made into a series of box diagrams, as shown in Figure 12. Whether the material is coal or gangue, under the condition of the same shape, the vibration signal caused by the rock impacting the tail beam at different angles has obvious discreteness, which is related to the unevenness of the surface characteristics of the rock and the difference in the landing posture. However, the vibration signals of the two materials have the same trend between the particles, showing that although the material changes and the strength of the response will change, for a certain shape of particles, the distribution of vibration response caused by the impact of the tail beam at different angles has a certain similarity.

Compared with the results of the same shape of different materials, the distribution of the vibration response data of the tail beam caused by coal is more concentrated, and the concentration of the acceleration is significantly higher than the concentration of the speed because the strength of the coal is less than the strength of the gangue, and a large amount of crushing occurs after the impact of the coal and the tail beam. After the collision, the contact state of the coal and the tail beam becomes surface contact, and the sensitivity of the vibration response signal to the initial contact shape and particle posture is reduced. Due to the small degree of fragmentation, the response caused by gangue is highly sensitive to the initial contact state. After the multiangle impact of the tail beam, the vibration signal caused by coal and gangue will indeed have discreteness, which

https://doi.org/10.1021/acsomega.1c06279
ACS Omega 2022, 7, 3656−3670

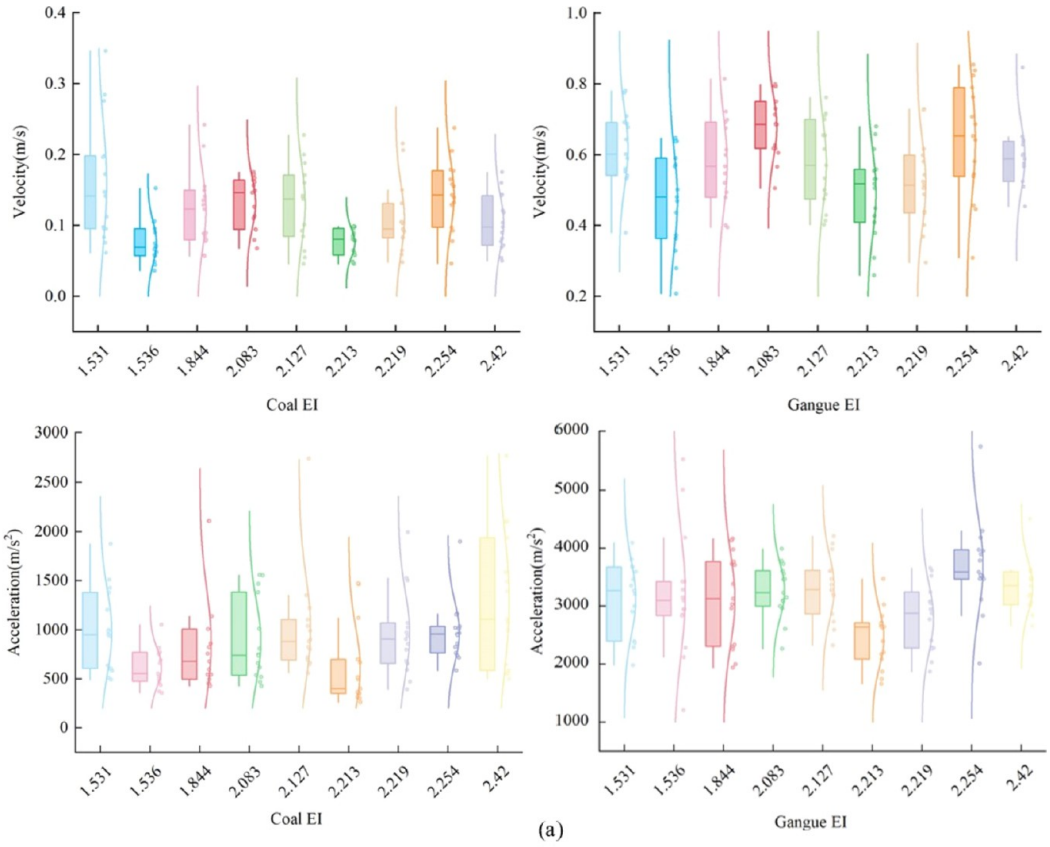

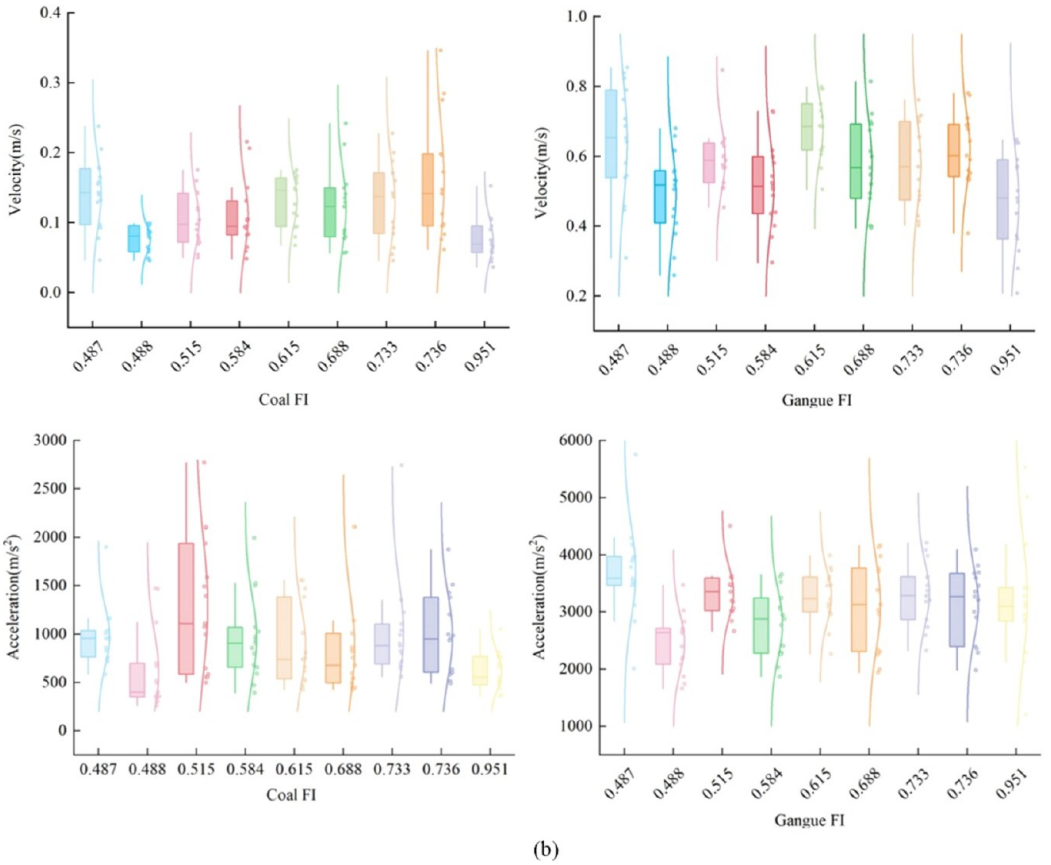

Figure 13. continued

https://doi.org/10.1021/acsomega.1c06279
ACS Omega 2022, 7, 3656−3670

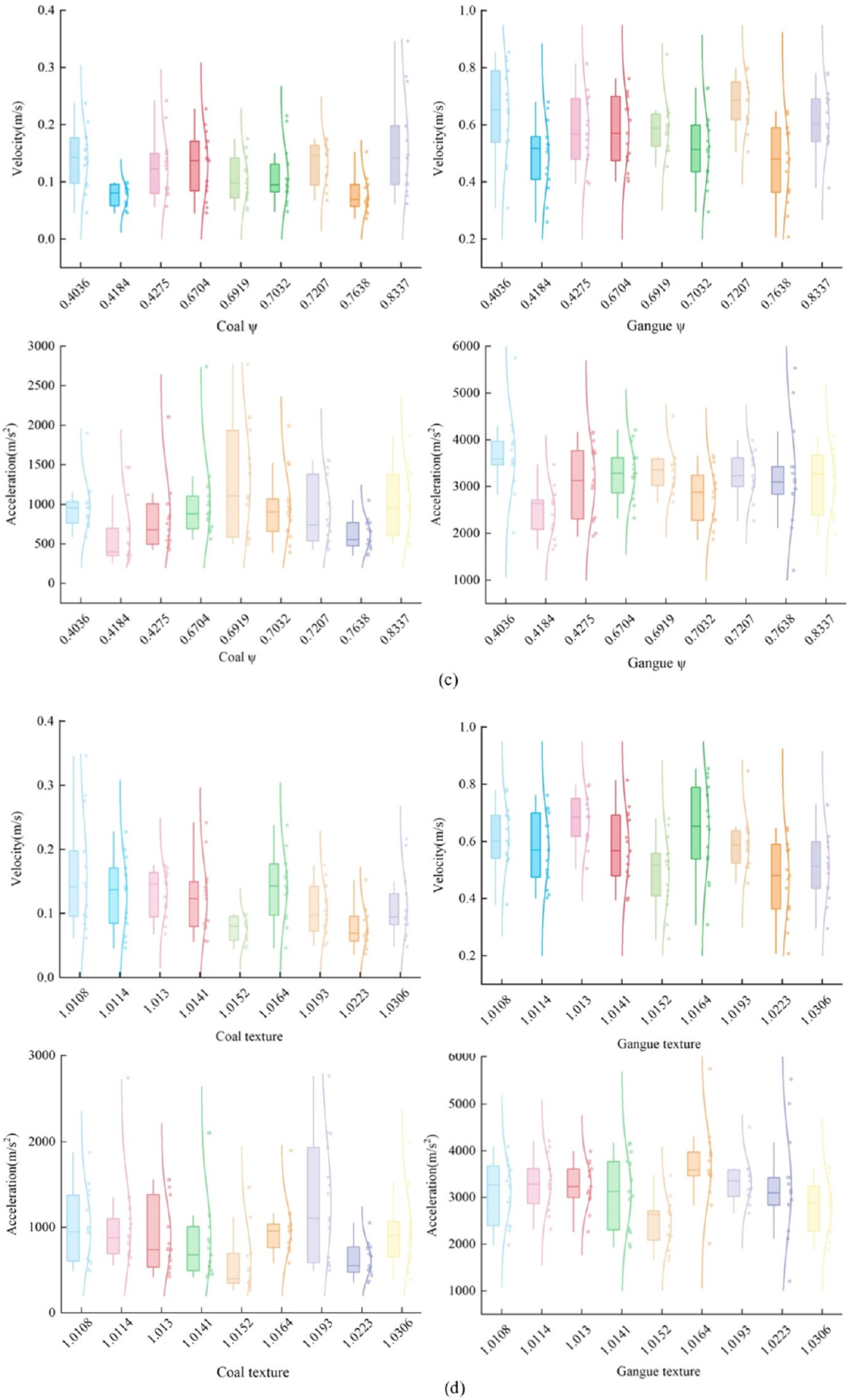

Figure 13. continued

https://doi.org/10.1021/acsomega.1c06279
ACS Omega 2022, 7, 3656−3670

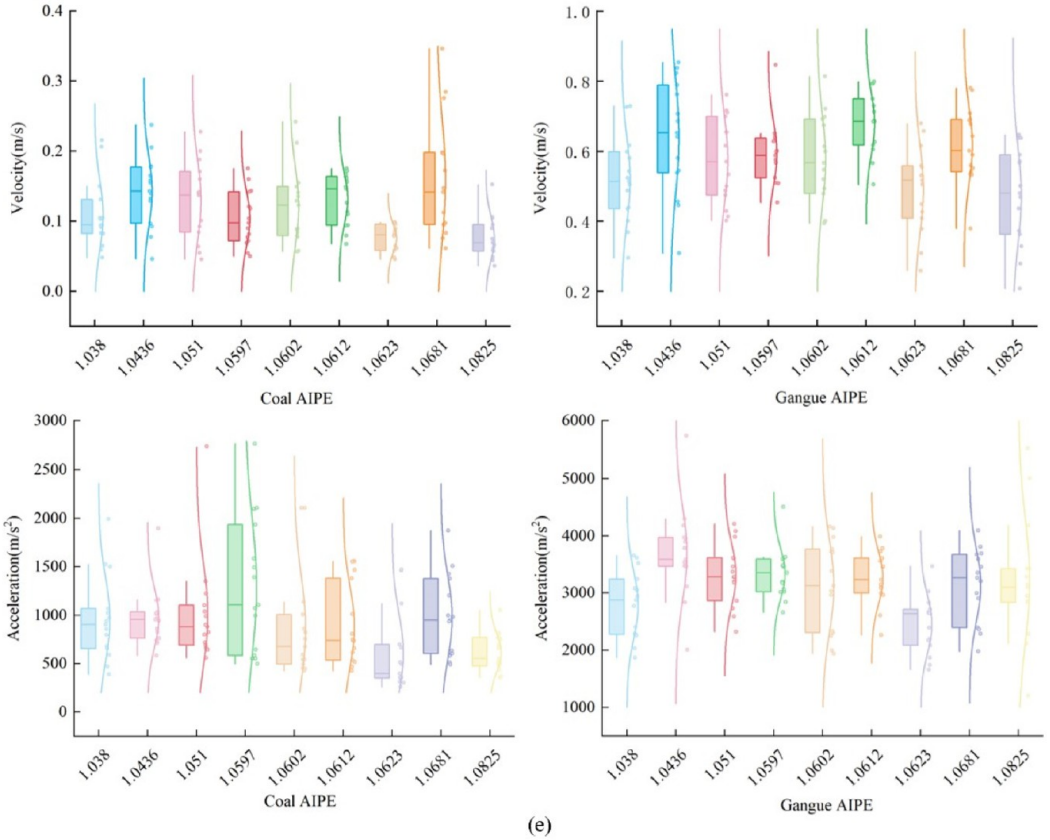

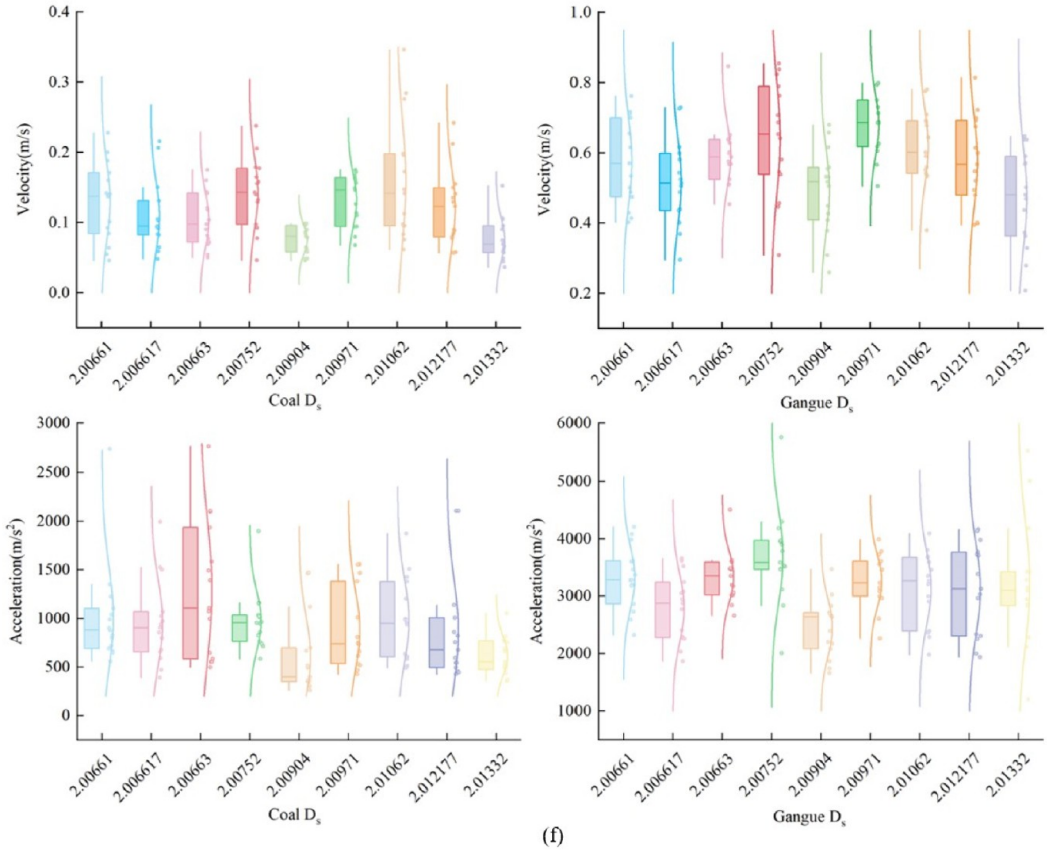

Figure 13. Influence of shape parameters on response data. (a) EI, (b) FI, (c) ψ, (d) texture, (e) AIPE, and (f) D_s.

https://doi.org/10.1021/acsomega.1c06279
ACS Omega 2022, 7, 3656−3670

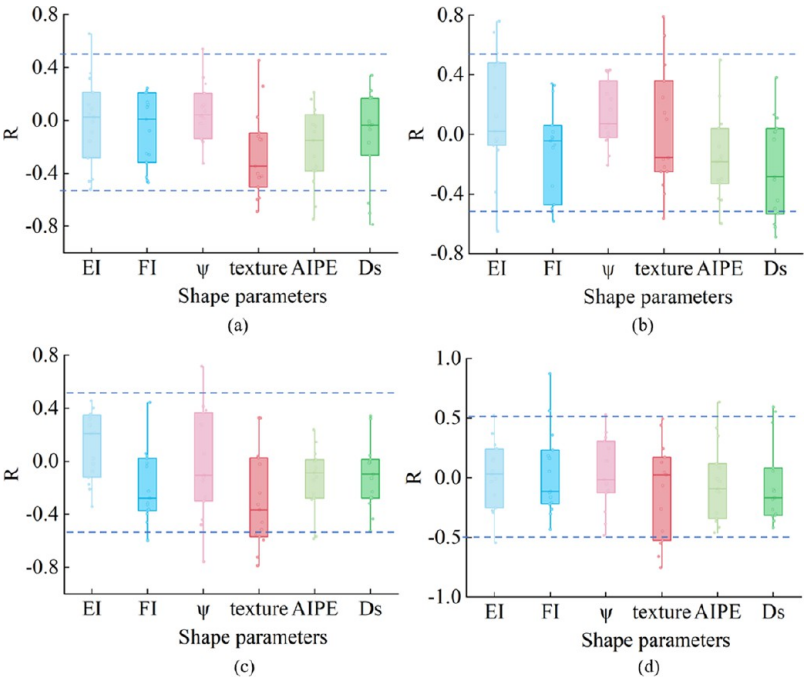

Figure 14. Correlation between shape parameters and vibration response of coal and gangue. (a) Velocity response of coal, (b) acceleration response of coal, (c) velocity response of gangue, and (d) acceleration response of gangue.

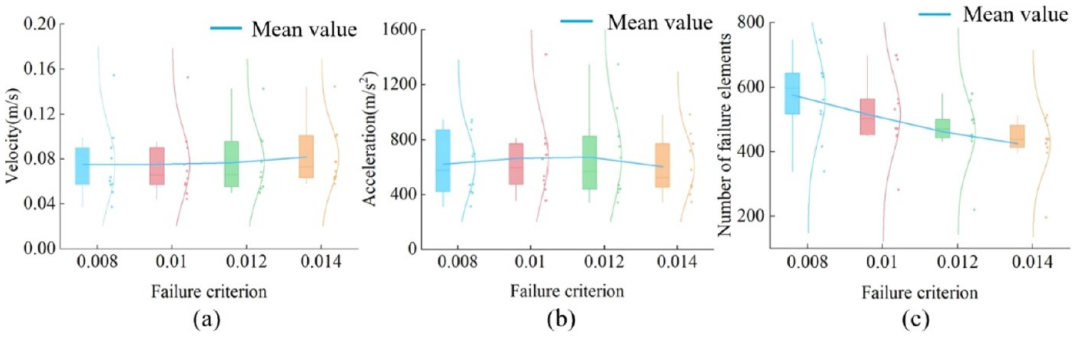

Figure 15. Effect of coal strength on the vibration. (a) Velocity, (b) acceleration, and (c) number of failure elements.

is consistent with the results of the simulation test of the ideal shape and the real shape of the particle impact on the metal plate, but the discreteness of the gangue is greater than the discreteness of the coal. Therefore, in the study of coal and gangue identification methods based on vibration, the degree of discretion of the vibration signal can be further studied as the basis for the distinction between coal and gangue, especially the acceleration signal.

4.3. Response and Shape Parameters. Figure 13 shows the results of sorting each particle with the shape parameter as the abscissa. The results show that a single shape parameter does not have a significant impact on the change trend of the response of the tail beam, and the response results show disorder. There may be two reasons for this result. One reason is that the number of particles in the test and the number of tests for each rock are relatively small, and the selection of particles is also accidental, resulting in uneven distribution of shape parameters. The other reason is that the vibration signal is affected by the surface shape characteristics and falling attitude of rock particles, which are affected by many factors.

The correlation between the shape parameters and each result in fifteen numerical simulation tests was analyzed, and the results are shown in Figure 14. The correlation coefficient of each shape parameter varies over a large range, and most of the correlation coefficients are less than ±0.5, indicating that the correlation between a single shape parameter and the velocity and acceleration response results is small, and the acceleration and velocity response are not affected by a single shape parameter.

In the process of top-coal caving mining, the coal particles in contact with the tail beam are often large and dense. Although the shape of each particle is different, we can consider that the distribution of various shape parameters should be constant in the coal particles covered on the tail beam at different times. Therefore, we speculate that the overall level of the vibration signal in the process of coal caving should be relatively stable and will not cause great disturbance to the signal due to the continuous change in the shape of coal gangue particles.

4.4. Study of Influence Factors. *4.4.1. Strength of Coal.* The strength of the coal under different geological conditions is also different. When the strength of the coal is low, the degree of crushing of coal will become larger. To further study the influence of coal strength on the vibration signal, the strength of coal is controlled by the failure criterion in the keyword * MAT _ ADD _ EROSION. The failure criterion is set to 0.008, 0.01,

https://doi.org/10.1021/acsomega.1c06279
ACS Omega 2022, 7, 3656−3670

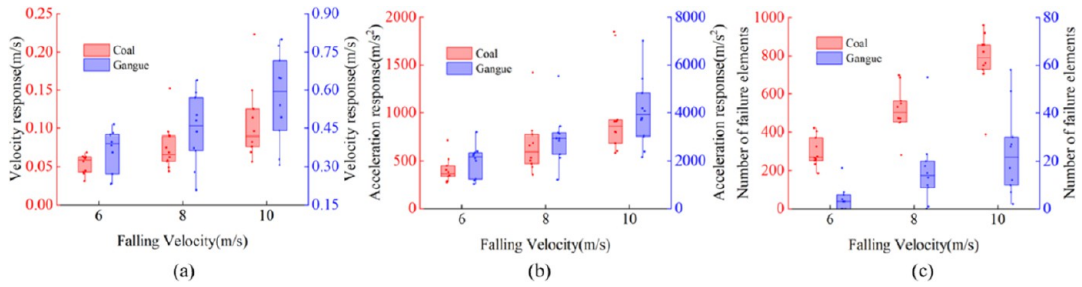

Figure 16. Effect of the falling velocity of rock particles on the vibration response. (a) Velocity response, (b) acceleration response, and (c) number of failure elements.

0.012 and 0.014. An increase in the number means an increase in coal strength. The falling speed is set to 8 m/s, and each parameter is simulated ten times. The same order of tests keeps other settings the same.

The change in coal strength directly affects the degree of coal crushing. The number of elements deleted due to coal failure in the first 0.01 s in each experiment is counted. Figure 15a shows that based on statistical analysis, the number of failure elements after coal impacts the tail beam decreases with the increasing failure standard. The results show that crushing decreases with increasing coal strength, conforming to the actual situation of coal gangue impacting hydraulic support.

The velocity and acceleration signals of the first collision area were extracted, and the effective values within 0.01 s were calculated. Figure 15a shows the influence of the strength change on the velocity response of the tail beam. The average velocity response results are 0.075, 0.0754, 0.0767, and 0.0818 under the four kinds of strength, and the rising trend is slow. As the strength increases, the contact stiffness of coal increases, the energy consumed by coal crushing decreases, and more energy is transferred to the tail beam, so the strength of the velocity response increases.

Figure 15b shows the relationship between the strength of coal and the acceleration response of the tail beam. Different from the change rule of velocity, the acceleration response has no obvious correlation with the strength, and the average values of each group are 619.77, 865.79, 671.87, and 601.52. The acceleration response of a node on the tail beam is possibly related to the contact force between the coal and the tail beam. The size of the contact force is related to the curvature radius, contact area, and elastic modulus of the coal. Because the process of coal contacting the tail beam and breaking is full of randomness, the parameters affecting the size of the contact force change randomly. At the same time, because the time of the crushing process in the contact process of the coal and tail beam has a certain influence on the signal intensity in the sampling time, the higher the strength of the coal is, the shorter the crushing process, and the signal intensity is weakened to some extent.

We can speculate that the strength of coal has little influence on the vibration signal. When the velocity or acceleration sensor is used to collect the vibration signal on the tail beam of the hydraulic support, it will not have a great influence on the identification of coal and gangue due to the different strengths of coal caused by different geological conditions in different mining areas. Therefore, the coal and gangue identification technology based on vibration analysis may be suitable for mining areas with different geological conditions.

4.4.2. Falling Velocity. To study the influence of the falling velocity on the vibration response of the tail beam, coal and gangue particles impacting the tail beam of the support with the same mass and surface morphology were tested. The mass is 13 kg, and the speed is 6, 8, and 10 m/s.

The test results are shown in Figure 16c. With increasing speed, the number of deleted elements of coal and gangue shows a significant upward trend, and the dispersion degree of the distribution of the results also increases. This result is basically consistent with the actual situation. With increasing speed, the contact force between the coal gangue particles and the tail beam will possibly increase, resulting in an increase in the degree of fragmentation. The contact depth of the coal gangue particles and the tail beam increases, the eroded part develops from the tip of the surface protrusion to the larger bottom, and the eroded volume of the particles rises rapidly. Due to the different initial states of different contact angles, the degree of dispersion of the data will be amplified as the speed increases.

Figure 16a,b shows the influence of the falling velocity of coal and gangue on the velocity and acceleration response. With increasing falling velocity, the discreteness of the response results of the tail beam caused by coal and gangue increases, indicating that the vibration response of the tail beam is sensitive to velocity. The average value of the six points in the middle position is calculated, and the difference between coal and gangue is found to be affected by either the velocity response or the acceleration response. When the falling velocities are 6, 8, and 10 m/s, the velocity response of gangue is 5.38, 4.77, and 4.69 times the velocity response of coal, and the acceleration response of gangue is 6.44, 6.62, and 6.11 times the acceleration response of coal, respectively. Considering the randomness of the finite element dynamic simulation results, we should consider that the difference between the two is also gradually reduced possibly because the increase in speed increases the time of the coal crushing process and strengthens the signal intensity in the first 0.01 s, while the contact time of gangue with the tail beam is almost unchanged due to the small degree of crushing. Therefore, in mining areas with lower coal caving heights, the coal gangue identification method based on vibration may have a higher degree of coal gangue identification.

5. CONCLUSIONS

To understand the real shape of the coal gangue particle impact beam caused by the signal and the difference between the signals, this paper uses the 3D scanning technology to determine the shape of the coal. The finite element model of coal gangue particles impacting hydraulic support tail beams was established in LS-DYNA, and the reliability of the simulation model was verified by a coal falling test. Compared with spherical particles, the vibration signal of the tail beam caused by the real shape of coal gangue particles presents obvious irregular variation characteristics. The influence differences of coal gangue particle

https://doi.org/10.1021/acsomega.1c06279
ACS Omega 2022, 7, 3656−3670

shape parameters, drop velocity, and material strength on tail beam vibration were studied. The following conclusions can be drawn.

1 After coal gangue impacts the tail beam of the hydraulic support, the vibration response of the tail beam is distributed mainly in the area between the two rib plates, which provides a reference for the arrangement of sensors. The tail beam velocity fluctuation caused by gangue is higher than the tail beam velocity fluctuation caused by coal, and the regularity of velocity attenuation caused by gangue is significantly higher the regularity of velocity attenuation caused by coal. The acceleration fluctuation caused by gangue will remain at a high level for a long time, while the acceleration fluctuation caused by coal will decay quickly.

2 The velocity and acceleration signals of coal obey lognormal distributions, while the velocity and acceleration signals of gangue obey gamma and Weibull distributions, respectively. The standard deviations of the velocity response of the tail beam caused by coal and gangue are 0.05591 and 0.13531, respectively, while the standard deviations of acceleration are 489.8 and 737.9, respectively. Therefore, the sensitivity of the vibration signal caused by gangue to the initial contact state is higher than the sensitivity of the vibration signal caused by coal.

3 There is no obvious regularity between the response results of a single shape parameter and different particles. Since the coal gangue particles are dense and large in the caving process of top coal caving, the influence of the shape change of coal gangue particles on the discrimination of coal gangue can be ignored.

4 The vibration response changes caused by coal particles with different strengths impacting the tail beam are weak. Therefore, coal gangue identification based on the tail beam vibration response has good adaptability to coal seam hardness.

5 When the velocity is between 6 and 8 m/s, the vibration response signal intensity of the tail beam increases with increasing velocity of coal gangue particles impacting the tail beam, but the discrimination of the vibration response decreases with increasing velocity.

At present, the method of measuring particle shape is not sufficiently accurate, and the process of coal gangue particles impacting hydraulic support is very complex. In future work, we will further study and explain the above problem through a better separation of influencing factors and more simulation tests.

In this study, the response difference between coal gangue particles was studied in a more realistic way. The results provide a reference for further study of coal gangue identification in top coal caving mining based on tail beam vibration signals.

AUTHOR INFORMATION

Corresponding Author

Zhaosheng Meng − *State Key Laboratory of Mining Disaster Prevention and Control Cofounded By Shandong Province and the Ministry of Science and Technology, Shandong University of Science and Technology, 266590 Qingdao, China*; Email: skdmzs@163.com

Authors

Lirong Wan − *College of Mechanical and Electronic Engineering, Shandong University of Science and Technology, Qingdao 266590, China*

Jiantao Wang − *College of Mechanical and Electronic Engineering, Shandong University of Science and Technology, Qingdao 266590, China*; orcid.org/0000-0002-2003-2072

Qingliang Zeng − *College of Mechanical and Electronic Engineering, Shandong University of Science and Technology, Qingdao 266590, China; College of Information Science and Engineering, Shandong Normal University, Jinan 250358, China*

Dejian Ma − *College of Mechanical and Electronic Engineering, Shandong University of Science and Technology, Qingdao 266590, China*

Xuehui Yu − *College of Mechanical and Electronic Engineering, Shandong University of Science and Technology, Qingdao 266590, China*

Complete contact information is available at: https://pubs.acs.org/10.1021/acsomega.1c06279

Notes

The authors declare no competing financial interest.

ACKNOWLEDGMENTS

This work was supported by National Natural Science Foundation of China (grant nos. 51974170 and 52104164), Key Research and Development of Shandong Province Exploration and Mining of Deep Resources (grant no. 2019SDZY01), and Natural Science Foundation of Shandong Province (grant no. ZR2019MEE067 and ZR2020QE103).

REFERENCES

(1) Sun, Z.; Huang, B.-X.; Li, Y.-H.; Lin, H.-R.; Shi, S.-Z.; Yu, W.-C. Nanoconfined methane flow behavior through realistic organic shale matrix under displacement pressure: a molecular simulation investigation. *J. Pet. Explor. Prod. Technol.* **2021**, DOI: 10.1007/s13202-021-01382-0.

(2) Yu, P.; Dempsey, D.; Archer, R. A three-dimensional coupled thermo-hydro-mechanical numerical model with partially bridging multi-stage contact fractures in horizontal-well enhanced geothermal system. *Int. J. Rock Mech. Min. Sci.* **2021**, *143*, 104787.

(3) Li, X.; Cao, Z.; Xu, Y. Characteristics and trends of coal mine safety development. *Energy Sources, Part A Recovery, Util. Environ. Eff.* **2020**, No. 12, 1−19.

(4) Liu, S.; Li, X.; Wang, D.; Zhang, D. Experimental Study on Temperature Response of Different Ranks of Coal to Liquid Nitrogen Soaking. *Nat. Resour. Res.* **2020**, *30*, 1467−1480.

(5) Zhao, J.-H.; Chen, J.-T.; Xing, H.-L.; Zhao, Z.-H.; Zhang, X.-G. Dynamic Mechanical Response and Movement Evolution Characteristics of Fault Systems in the Coal Mining Process. *Pure Appl. Geophys.* **2021**, 2905−2913.

(6) Ma, D.; Zhang, X.; Wan, L.-R.; Zeng, Q.-L.; Ge, H.-E. Dynamic Analysis of Shearer Traction Unit Considering the Longitudinal Swing. *Energies* **2020**, *13*, 5293.

(7) Alehossein, H.; Poulsen, B. A. Stress analysis of longwall top coal caving. *Int. J. Rock Mech. Min. Sci.* **2010**, *47*, 30−41.

(8) Zhang, S.-X.; Zhang, X.-L.; Liu, S.; Xu, G.-Q. Intelligent precise control technology of fully mechanized top coal caving face. *Mei Tan Xue Bao* **2020**, *45*, 2008−2020.

(9) Wang, W.; Zhang, C. Separating coal and gangue using three-dimensional laser scanning. *Int. J. Miner. Process.* **2017**, *169*, 79−84.

(10) Dou, D.; Wu, W.; Yang, J.; Zhang, Y. Classification of coal and gangue under multiple surface conditions via machine vision and relief-SVM. *Powder Technol.* **2019**, *356*, 1024−1028.
(11) Duan, Y. Research and realization identification and positioning method of coal and gangue based on image. Master dissertation, Xi'an University of Science and Technology, Beijing, 2020.
(12) Li, M.; Duan, Y.; Cao, X.-G.; Liu, C.-Y.; Sun, K.-K.; Liu, H. Image identification method and system for coal and gangue sorting robot. *Mei Tan Xue Bao* **2020**, *45*, 3636−3644.
(13) Li, Y.-M. Collapsing coal and rock recognition method based on non−stationary vibration signal in fully mechanized caving face. Beijing. Doctoral dissertation, China University of Mining & Technology, Beijing, 2018.
(14) Zhang, N.; Liu, C. Radiation characteristics of natural gamma-ray from coal and gangue for recognition in top coal caving. *Sci. Rep.* **2018**, *8*, 190.
(15) Zeng, Q.; Yang, Y.; Zhang, X.; Wan, L.; Zhou, J.; Yin, G. Study on Metal Plate Vibration Response Under Coal-Gangue Impact Based on 3D Simulation. *Arabian J. Sci. Eng.* **2019**, *44*, 7567−7580.
(16) Li-rong, W.; Chen, B.; Yang, Y.; Yin, G.-J.; Li, R.; Zeng, Q.-L. Research on response of coal gangue particles collision based on adams. *Coal Technol.* **2018**, *37*, 236−239.
(17) Wan, L.-R.; Yin, G.-J.; Yang, Y.; Li, R.; Zeng, Q.-L. Study on vibration characteristics of single granular rock direct impact metal plate. *Coal Technol.* **2017**, *36*, 213−216.
(18) Wan, L. R.; Chen, B.; Yang, Y.; Zeng, Q. L. Dynamic response of single coal-rock impacting tail beam of top coal caving hydraulic support. *Mei Tan Xue Bao*. **2019**, *44*, 2905−2913
(19) Yan, P.; Zhang, J.; Fang, Q.; Zhang, Y. Numerical simulation of the effects of falling rock's shape and impact pose on impact force and response of RC slabs. *Constr. Build. Mater.* **2018**, *160*, 497−504.
(20) Xie, W.-Q.; Zhang, X.-P.; Yang, X.-M.; Liu, Q.-S.; Tang, S.-H.; Tu, X.-B. 3D size and shape characterization of natural sand particles using 2D image analysis. *Eng. Geol.* **2020**, *279*, 105915.
(21) Lu, G.; Ringenbach, A.; Caviezel, A.; Sanchez, M.; Christen, M.; Bartelt, P. Mitigation effects of trees on rockfall hazards: does rock shape matter? *Landslides* **2020**, *18*, 59−77.
(22) Wang, S.; Cheng, G.-X.; Zhang, L.-K.; Yuan, J. Triaxial discrete element simulation of soil−rock mixture with different rock particle shapes under rigid and flexible loading modes. *Int. J. GeoMech.* **2021**, *21*, 04021142.
(23) Yan, P.; Zhang, J.-H.; Kong, X.-Z.; Fang, Q. Numerical simulation of rockfall trajectory with consideration of arbitrary shapes of falling rocks and terrain. *Comput. Geotech.* **2020**, *122*, 103511.
(24) Su, Y.; Choi, C. E. Effects of particle shape on the cushioning mechanics of rock-filled gabions. *Acta Geotech* **2020**, *16*, 1043−1052.
(25) Li, R.-Z.; Lu, W.-B.; Yin, Y.-J.; Yu, Y.-J.; Chen, M.; Xia, W.-J.; Yan, P. Study on the shape and specific surface area characteristics of blasting gravel particles of limestone in Hangudi quarry of Baihetan. *Chin. J. Rock Mech. Eng.* **2019**, *38*, 1344−1354.
(26) Zhang, J.-Q.; Wang, X.; Yin, Z.-Y.; Liang, Z.-Y. DEM modeling of large-scale triaxial test of rock clasts considering realistic particle shapes and flexible membrane boundary. *Eng. Geol.* **2020**, *279*, 105871.
(27) Zhou, J.; Ma, G.; Zhou, W.; Cheng, Y.-G.; Huang, Q.-S.; Cao, X.-X. Statistical analysis of fragment shape of rock grain after crushing based on FDEM. *J. Zhejiang Univ. Eng. Sci.* **2021**, *55*, 348−357.
(28) Wan, L.-R.; Chen, B.; Yang, Y.; Zeng, Q.-L. Study on Dynamic response of single coal-rock impacting tail beam of top coal caving hydraulic support. *Mei Tan Xue Bao* **2019**, *44*, 2905−2913.
(29) LS-DYNA. *Keyword User's Manual*; Livermore software technology corporation, 2016; Vol. *2*.
(30) Yang, Z.-Y. Research on Impact Crushing in Luna Soil Sampling Based on ANSYS/Ls-dyna Numerical Simulation. Master dissertation, Harbin Institute of Technology, Harbin, 2019.
(31) Liu, B.; Yang, S.-Z.; Li, W.-L.; Zhang, M.-Q. Damping dissipation properties of rubberized concrete and its application in anti-collision of bridge piers. *Constr. Build. Mater.* **2020**, *236*, 117286.
(32) Liu, K.; Wu, C.-Q.; Li, X.-B.; Li, Q.-Y.; Fang, J.-G.; Liu, J. A modified HJC model for improved dynamic response of brittle materials under blasting loads. *Comput. Geotech.* **2020**, *123*, 103584.
(33) Li, Y. Researches on HJC Dynamic Constitutive Model for Concrete. Master dissertation, Hefei University of Technology, Hefei, 2009.
(34) Long, X.; Turgun, A.; Yue, R.; Ma, Y.; Luo, H. Influence Factors Analysis of RC Beams under Falling Weight Impact Based on HJC Model. *Shock Vib.* **2018**, *2018*, 1−16.
(35) Xie, B.-J. Experimental Research on Characteristics of Coal Impact Damage Dynamics and Magnetic Field. Beijing. Master dissertation, China University of Mining & Technology, Beijing, 2013.

https://doi.org/10.1021/acsomega.1c06279
ACS Omega 2022, 7, 3656−3670